6-1-2021

Detecting Change in Precipitation Indices Using Observed (1977-2016) and Modeled Future Climate Data in Portland, Oregon, USA

Alexis Kirsten Cooley
Portland State University

Heejun Chang
Portland State University, changh@pdx.edu

Citation Details

Cooley, A. K., & Chang, H. (2021). Detecting change in precipitation indices using observed (1977–2016) and modeled future climate data in Portland, Oregon, USA. *Journal of Water and Climate Change*, *12*(4), 1135–1153. https://doi.org/10.2166/wcc.2020.043

Detecting change in precipitation indices using observed (1977–2016) and modeled future climate data in Portland, Oregon, USA

Alexis Kirsten Cooley and Heejun Chang

ABSTRACT

This study addresses how regional changes to precipitation may be identified by exploring the effect of temporal resolution on trend detection. Climate indices that summarize precipitation characteristics are used with Mann–Kendall monotonic testing to investigate precipitation trends in Portland, Oregon (OR) from 1977 to 2016. Observational records from rain gages are compared with downscaled global climate models to determine trends for the historic (1977–2005) and future (2006–2100) periods. Standard indices created by the Expert Team on Climate Change Detection and Indices (ETCCDI) are deployed. ETCCDI indices that summarize conditions at the annual level are generated alongside a limited number of ETCCDI indices summarized at the monthly level. For the future climate, the indices summarized at the annual level demonstrate trends indicative of an intensifying hydrologic cycle. The historical record depicted by annual indices does not show trends. The historical record is viewed differently by changing the indices to monthly summaries, which causes trend detection to increase and hallmark indicators of an intensifying hydrologic cycle to become apparent.

Key words | ETCCDI precipitation indices, global climate models, hourly precipitation, scale, trend

Alexis Kirsten Cooley
Heejun Chang (corresponding author)
Department of Geography,
Portland State University,
1721 SW Broadway, Portland, OR 97201,
USA
E-mail: *changh@pdx.edu*

HIGHLIGHTS

- We used the Expert Team on Climate Change Detection and Indices (ETCCDI) precipitation indices and the Mann–Kendall test to detect trends in precipitation.
- We compared observed precipitation records (1977–2005) with future (2006–2100) projections from five downscaled global climate models for the Portland area.
- While four of five climate models projected an intensifying hydrologic cycle from 2006 to 2100, trends were not detected in the 1977–2016 observational record.
- When data were disaggregated from annual to monthly, many of the hallmarks of an intensified hydrologic cycle were observed in the 1977–2016 Portland record in spring, winter, and fall months.
- Trend detection of increasing precipitation intensity was detected more at a finer temporal scale (i.e., hourly data), indicating a finer temporal analysis is critical for urban flood risk management.

doi: 10.2166/wcc.2020.043

GRAPHICAL ABSTRACT

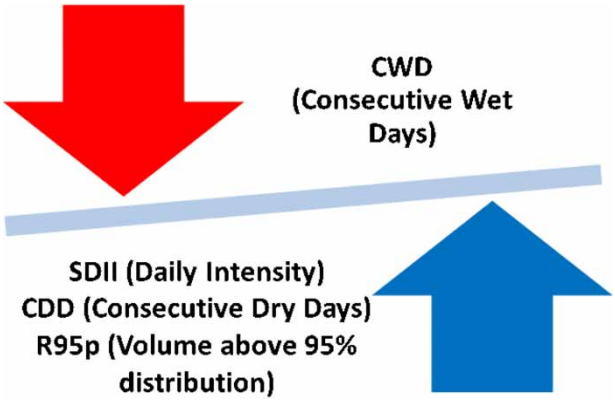

INTRODUCTION

As a consequence of rising levels of greenhouse gases, the global hydrologic cycle is likely to intensify (Huntington 2006). Changes to patterns of precipitation are confidently expected in part because a warmer atmosphere can hold additional water vapor, as described by the Clausius–Clapeyron model of gas behavior under conditions of temperature increase. The effects of temperature rise on precipitation can vary but include the possibilities for altered routes of water vapor transport in atmospheric circulation and different seasonal precipitation patterns (Held & Soden 2006; Wentz *et al.* 2007; Trenberth 2011).

Global shifts in precipitation regime are expected to already be occurring because global temperature rise is highly certain (IPCC 2013). An increase in atmospheric water vapor has been observed globally, and some studies suggest changes in tropical and sub-tropical rainfall cannot be explained without a global greenhouse gas (GHG) signal (Hense *et al.* 1988; Zhang *et al.* 2007). Many other precipitation trends have been detected around the world, but with varying periods of study and measurement techniques, these studies may be site-specific rather than connected by the underlying warming trend (Groisman *et al.* 1999, 2005; Osborn *et al.* 2000; Krishnamurthy *et al.* 2009; Soulis *et al.* 2016).

It is important to consider regional and seasonal changes in precipitation in order to identify emerging change to the hydrologic cycle. Changes in the seasonal distribution of precipitation could affect drinking water resources in regions where reservoirs rely on snowmelt filling (Barnett *et al.* 2008). Decreased rain in the arid regions of the Middle East and Northern Africa can lead to failed harvests and disruption of the agricultural sector (Dai 2011; Homsi *et al.* 2020). Although mean precipitation increased in mid-latitude land areas since 1951, trends at other latitudes are less confident (IPCC 2013). This is evidence of the need for regional studies and the inadequacy of using a single metric for the entire globe.

Many studies of regional precipitation exist but do not lend themselves to a clear narrative about climate change because of widely varied research methods and results reporting (Moberg *et al.* 2006). The development of common metrics for measuring change to precipitation and other weather variables can improve communication and cooperation. In response to such needs, scientific communities created a number of common indices. These indices include the Expert Team on Climate Change Detection and Indices (ETCCDI) and also the Expert Team on Sector-specific Climate Indices (ET-SCI), both of which emerged from the World Meteorological Organization (WMO) (Zhang *et al.* 2011). The European Climate Assessment & Dataset (ECA&D) created further indices (Klok & Klein Tank 2009). Many of the indices sets are appropriate for different contexts. Sector-specific indices were the basis for ET-SCI and may be applied to the

industries of agriculture, health, and water resources. Not all indices may be appropriate for any region. Some drought indices may outperform others depending on the region, and evaluating fitness to the region is often appropriate (Shamshirband *et al.* 2020).

The ETCCDI indices are aimed at global ubiquity and have been adopted in studies of many regions. Reviews of regional studies employing ETCCDI indices shown in Table 1 demonstrate consistent temperature increase and disparate precipitation trends around the globe. Although trends were found in precipitation indices like rainfall intensity (SDII) and precipitation total (PRCPTOT), trends are not consistently positive or negative. There is a distinct lack of clarity on the mechanisms creating spatially incoherent trends. Increases to intensity (SDII) and maximum single-day rainfall (Rx1day), which can potentially affect the magnitude of runoff and the intensity of the hydrologic cycle, are present in many studies, but these trends are rarely consistent across the entire study area (Rahimzadeh *et al.* 2009; Dumitrescu *et al.* 2015).

Temporal scale is another important feature in the study of precipitation, and current ETCCDI methodology does not dictate multiple scales of analysis. The RClimDex software widely employed by researchers to calculate ETCCDI indices is designed so that the period of study is annual, although monthly calculations are available for some indices (Zhang & Yang 2004). Many researchers have opted to conduct research on an annual or seasonal basis, and a few have used monthly (Table 1). Further, ETCCDI indices are based on the use of daily precipitation and temperature data. Considering that modern precipitation research can now look at sub-daily rain rates through innovations in remote sensing and computation, the use of the daily scale may be limiting (Munoz *et al.* 2015; Sanò *et al.* 2015).

Further, the use of daily records obscures the fact that precipitation is a phenomenon occurring at a sub-daily scale (Trenberth 1998). Daily data have been shown to mask trends in precipitation intensity when compared to sub-daily data (Cooley & Chang 2017). It is possible that the use of annual time scales and daily data may contribute to the incoherent precipitation trends observed. One reason for the use of daily data in the ETCCDI indices is that the indices are designed to emphasize global collaboration and high-resolution records are not available in many regions (Peterson & Manton 2008). Further, ETCCDI indices are not only used for historical analysis but also for future projections made by global climate models. Although the resolution of climate models steadily increases, the ability of these models to deliver precipitation projections that resemble realistic precipitation at the hourly scale remain novel (Xu *et al.* 2005; Seneviratne *et al.* 2006; Prein *et al.* 2016).

The atmospheric dynamics that lead to precipitation in the Pacific Northwest are expected to be altered by climate change (Chou *et al.* 2012; Rupp *et al.* 2017a, 2017b). The results of this include an intensification of convergence zones like the North Pacific storm track that transport water vapor to the Pacific Northwest (Salathé 2006). Atmospheric rivers that are responsible for many of the flood events in the region are anticipated to increase in duration and frequency (Dettinger 2011). A regional climate model indicates an increased magnitude of single-day rainfall events in the twenty-first century (Salathé *et al.* 2014). Elevation increase of snow lines may contribute to increased precipitation if a greater portion of moisture falls as rain rather than snow (Tohver *et al.* 2014).

Annual precipitation has increased in the Pacific Northwest over the twentieth century, although whether this is attributable to climate change is debatable (Mote 2003). The seasonal distribution of the increased precipitation from climate change is expected to occur in winter, but most observed significant increasing trends are in spring (Abatzoglou *et al.* 2014). Global climate models predict annual mean precipitation changes of −10% to 20% by the 2080s for the Pacific Northwest (Mote 2003; Salathé 2006; Mote & Salathé 2010; Rupp *et al.* 2017a, 2017b). The seasonal distribution of precipitation is likely to skew towards winter months with summers becoming drier.

Although many studies have investigated the long-term climate change in the Pacific Northwest, hydrologic studies of observational records have tended to focus on streamflow, snowpack, and modes of climate variability (Chang *et al.* 2012). El Nino and the Pacific Decadal Oscillation have been shown to have an important influence over temperature but only moderate influences on precipitation (Redmond & Koch 1991; Praskievicz & Chang 2009).

A number of recent studies of precipitation have been conducted in British Columbia. Predictions of increased winter rainfall and decreased summer rainfall have not

Table 1 | Review of global literature using ETCCDI indices

Continent	Region	Years	Scale	Author	Summary
Asia	India	1901–2004	Annual	Panda *et al.* (2016)	Increase: SDII, R95pTOT (*annual precipitation in 95 percentile)*, R99pTOT (*annual precipitation in 99 percentile*). Decrease: CWD (monsoon region). No temperature indices used.
Asia	Indonesia	1983–2012	Seasonal	Tangang *et al.* (2017)	Increase: TX90p (*monthly max temperatures in 90 percentile)*, TN90p (*monthly min temperatures in 90 percentile*), SDII (winter/spring), Rx1Day (winter/spring). Decrease: SDII (summer, southern regions), Rx1day (summer, southern regions).
Asia	Iran	1951–2003	Annual	Rahimzadeh *et al.* (2009)	Increase: TX90p, TN90p, SDII (North region) Decrease: PRCPTOT (two-thirds of country)
Europe	Romania	1961–2013	Seasonal	Dumitrescu *et al.* (2015)	Increase: SU (*number summer days*), WSDI (*warm spell duration*), R10 mm (*annual count of days when precipitation greater than 10 mm),* (various sub-regions), R20 mm (*annual count of days when precipitation greater than 20 mm*), (various sub-regions), SDII (various sub-regions). Decrease: FD (*frost days*), SDII (various sub-regions).
Europe	Catalonia, Spain	1951–2003	Annual/ Seasonal	Turco & Llasat (2011)	Increase: CDD, PRCPTOT (summer), RX5Day (summer). No temperature indices used.
Africa	South Africa	1962–2009	Annual	Kruger & Sekele (2013)	Increase: TX90, TXx, TN90p. No precipitation indices used.
Africa	Morocco	1970–2012	Annual/ Seasonal	Filahi *et al.* (2016)	Increase: TX90p, TN90p, SDII (coastal regions). Decrease: PRCPTOT.
Australia	Australia	1930–2011	Monthly	King *et al.* (2014)	Increase: Rx5day (single sub-region). Only Rx5day tested, no other indices used.
South America	Paraná River Basin, Brazil	1986–2011	Annual	Zandonadi *et al.* (2016)	Increase: R95p, SDII, R20 mm, R10 mm. PRCPTOT. No temperature indices used.
South America	South America	1950–2010	Annual	de los Milagros Skansi *et al.* (2013)	Increase: TNn, TN90p, Rx1day, Rx5day, R95p, PRCPTOT, SDII. (Precipitation trends are concentrated in Amazonia and southeast regions).
North America	Northeast US States	1951–2010	Annual	Thibeault & Seth (2014)	Increase: R95pTOT, Rx1day, Rx5day, CWD. Decrease: TN10p (*Monthly min temperatures in 10 percentile)*.
North America	Tlaxcala, Mexico	1952–2003	Seasonal	Diaz *et al.* (2012)	Increase: FD, SU. Decrease: TX10p. No precipitation indices used.

yet been born out in studies of observational records (Burn & Taleghani 2013). Instead, increased frequency of heavy precipitation events in summer has been observed while winter has mixed signals. Some indication of increased intensity in spring has also been observed (Jakob *et al.* 2003). The nature and direction of trends are different across sub-regions, suggesting that different convective processes are creating diverse precipitation response. Examining the spatial extent of extreme precipitation in the Pacific Northwest, heterogeneous topography was found to be a key limiting factor on the spatial extent of extreme rainfall (Parker & Abatzoglou 2016). For this reason, closely related areas with different topography may have different responses to climate change, suggesting the need for a spatially explicit analysis.

The authors' initial work in the City of Portland explored how the lack of precipitation trends from GHG forcing could be explained by coarse data resolution, and that improved temporal resolution could improve trend detection (Cooley & Chang 2017). Limitations to the previous research included that the period of study was short-term (1999–2015) and only examined signals from precipitation intensity. The present study further investigates the lack of clarity on recent climate signals by examining how annual data resolution can mask many changes to climate characteristics. To accomplish this, a suite of climate trends were examined instead of only rainfall intensity; the period of study was expanded to 1977–2100; and trends were calculated using the common indexes created by ETCCDI for the purpose of greater standardization.

The following research questions are addressed:

1. Do ETCCDI climate measurements for observed precipitation in Portland, OR, fit historic or future climate model projections?
2. How does changing the study analysis unit from annual to monthly alter trend detection?
3. How does the use of daily instead of hourly records effect trend detection?

STUDY AREA

The City of Portland is located 129 km East of the Pacific Ocean in the lower Pacific Northwest, near the 45th parallel in the Northern Hemisphere (Figure 1). The Köppen–Geiger climate map describes it as a 'Csb' climate; temperate with

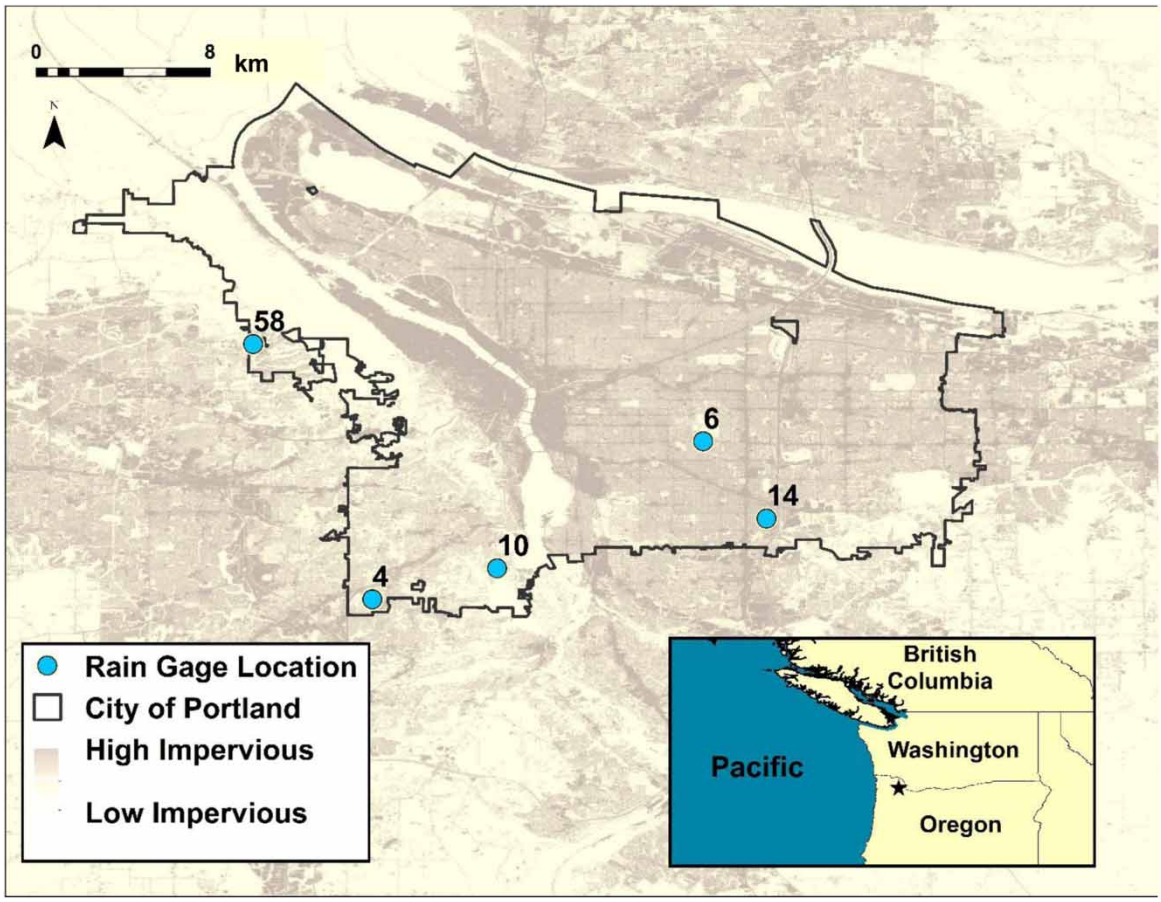

Figure 1 | Map of the study area.

warm, dry summers (Peel *et al.* 2007). Moisture is transported to the area through the North Pacific storm track (Dart & Johnson 1981). Regional precipitation distribution is highly variable and driven by complex topography and orographic lift (Salathé 2003). Portland is located in a low-lying area between the Coastal and Cascade mountain ranges and therefore receives relatively less precipitation than the surrounding mountains, around 930 mm of rain annually (based on years 1981–2010) (Chang 2007). The City of Portland was selected as the area of study because of a practitioner interest in exploring changes to rainfall and the availability of a high-resolution rainfall gage network suitable for studies of temporal resolution. With a potential increase in wet season rain and flooding in the future (Chang *et al.* 2010; Cooley & Chang 2017), changing rainfall patterns may require climate adaptation strategies. Additionally, as part of the Urban Resilience to Extremes Sustainability Resilience Network (UREx SRN), an international research network that seeks to improve urban resilience to extreme weather, academic researchers collaborated with city practitioners in improving the understanding, communication, and applications of climate change science (Grimm *et al.* 2018). During the period of 2015–2017, researchers from Portland State University explored how global warming may alter precipitation and how results could be effectively communicated to local wastewater and stormwater practitioners.

DATA AND METHODS

Data

Precipitation records with a 5-minute temporal resolution for the period of 1 January 1977 to 31 December 2016 were used from five rain stations in the City of Portland Hydrological Data Retrieval and Alarm (HYDRA) gage network. The forty-year period is sufficiently long enough to detect any changes to precipitation indices since the ENSO intensity has changed since the late 1970s (Wang *et al.* 2019). Recent data were not included because the researcher and practitioner collaboration that occurred under the UREx SRN for this project disbanded in 2017, with personnel changes. Data coverage is 95% complete. Figure 1 describes the location of these five rain gages. Using the Pandas package from Rv3.1.1, the data were summarized at the daily and hourly (0:00–23:59) resolution (R Core Team 2014). Inspection of data quality was performed visually by graphing time series data and manually identifying outliers outside three standard deviations of the mean. No precipitation outliers were identified. Temperature outliers were identified and examined, but no spurious points required removal.

In addition to observed historical climate data, simulated historical and projected future climate data were obtained from representative climate models. Climate model selection was based on superior performance, projecting accurate spatial and historic precipitation conditions in the Pacific Northwest during the twentieth century (Rupp *et al.* 2013). The focus on historical accuracy in the models favors the handling of short-range heterogeneous terrain rather than long-range circulations. It would be beneficial to deploy performance metrics to evaluate how well the simulations match the observed record (Burgan & Aksoy 2020). Several techniques exist to identify superior models that closely track observed records when regional accuracy is needed (Homsi *et al.* 2020). These likely create the best method to determine what future weather will look like, but this study is more focused on the scale of data and on communication than on being a perfect representation of future climate. This subject is recommended for future research, and this paper relies on the work of Rupp *et al.* (2013) who evaluated model accuracy. Five global climate models were chosen from the CMIP5 multi-model ensemble, CanESM2, CSIRO-Mk3.6.0, CNRM-CM5, HadGEM2-ES, and GFDL-ESM2M (Taylor *et al.* 2012). Table 2 shows the models and institutions responsible for development.

Downscaled daily precipitation projections were obtained using the Localized Constructed Analogs (LOCA) archive from the CMIP5 Climate and Hydrology Projections (Pierce *et al.* 2014). LOCA downscaling increases the global climate model grid resolution to $1/16^\circ \times 1/16^\circ$ horizontal latitude-longitude grid resolution (Pierce *et al.* 2014). A single Portland, OR grid point at 45.523°N, −122.677° W was selected for both historic projections (1977–2005) and future projections (2006–2100), except for the HadGEM2-ES model (2006–2099).

The Representative Concentration Pathway (RCP) 8.5 high emissions scenario was selected because the large

Table 2 | Global climate models used and the creator of each model

Model Name	Institute ID	Modeling Center
CanESM2	CCCMA	Canadian Centre for Climate Modelling and Analysis
CNRM-CM5	CNRM-CERFACS	Centre National de Recherches Météorologiques/Centre Européen de Recherche et Formation Avancée en Calcul Scientifique
CSIRO-Mk3.6.0	CSIRO-QCCCE	Commonwealth Scientific and Industrial Research Organization in collaboration with Queensland Climate Change Centre of Excellence
GFDL-ESM2M	NOAA GFDL	NOAA Geophysical Fluid Dynamics Laboratory
HadGEM2-ES	MOHC (additional realizations by INPE)	Met Office Hadley Centre (additional HadGEM2-ES realizations contributed by Instituto Nacional de Pesquisas Espaciais)

GHG forcing it uses relative to other CMIP5 scenarios provides a greater likelihood of detecting a GHG-forced signal. This scenario represents a future with a global population of 12 billion in 2100, where minimal gains from technological advances in energy efficiencies occur (Riahi *et al.* 2011). Selecting a study with weaker GHG forcing is less likely to show hydrologic change and less likely to represent actual conditions. RCP 8.5 is considered the most probable future considering the current rate of GHG emissions (Jackson *et al.* 2018).

Historical temperature records were 100% complete and were acquired from National Climatic Data Center (NCDC) Station 356751 located at Portland International Airport (PDX). Daily maximum and minimum temperature were obtained for 1977–2016.

Methods

Methods for Question 1: comparisons with downscaled climate models

Changes to the hydrologic cycle from climate change were hypothesized to show in aspects of the GHG-forced climate record. Precipitation indices that measure characteristics of rainfall were selected from ETCCDI. Giorgi *et al.* (2014) predicted that consecutive dry days (CDD) would increase and that rainfall events would be shorter, more intense, and wetter (Giorgi *et al.* 2011, 2014). Figure 2 shows the selected indices and hypotheses about the future state of these variables. Annual indices include simple daily rainfall intensity (SDII), maximum CDD, maximum consecutive wet days (CWD), and total days of precipitation above the 95th percentile (R95p). SDII, R95pTOT, CDD increase while CWD decreases. Table 3 presents the equations for these as defined by ETCCDI. Indices were selected based on a focus on regional precipitation and storm duration and intensity. These parameters are relevant to wastewater and stormwater engineering because of their use in design storm standards. This study presents less focus on indices, such as temperature that could be used to study the physical mechanisms driving hydrologic change.

The RClimDex software created by ETCCDI was used to generate the selected indices (Zhang & Yang 2004). The RClimDex software is designed to run parallel to the statistical software R. Input climate variables to the RClimDex software include daily precipitation, maximum temperature, and minimum temperature. The software uses these inputs to generate a unique index value for every year of the study. Alternatives to the RClimDex include ClimPact2 that also calculates several of the same indices. ClimPact2 is a more recently built software package and has the advantage of a new user interface and documentation. However, ClimPact2 is less well established in the literature. The

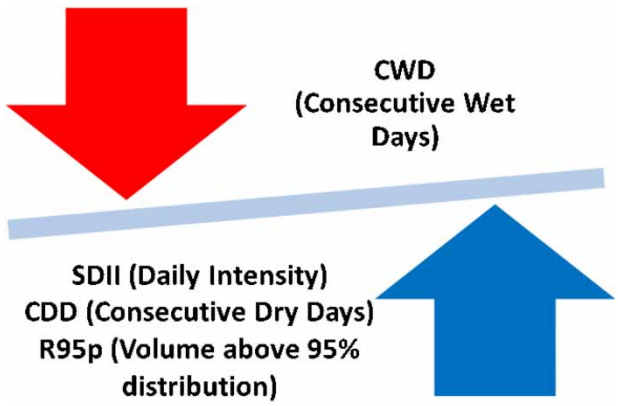

Figure 2 | Expected change to ETCCDI indices for 2006–2100 (Giorgi *et al.* 2014).

Table 3 | Definition of ETCCDI indices used for Research Question 1 (Karl *et al.* 1999; Peterson *et al.* 2001)

Indicator	Definition	Potential changes in the hydrological cycle
CDD (Equation (1))	Maximum length of dry spell, maximum number of consecutive days with RR <1 mm: Let RR_{ij} be the daily precipitation amount on day i in period j. Count the largest number of consecutive days where: $RR_{ij} < 1$ mm	Soil moisture, evapotranspiration rate
CWD (Equation (2))	Maximum length of wet spell, maximum number of consecutive days with RR ≥1 mm: Let RR_{ij} be the daily precipitation amount on day i in period j. Count the largest number of consecutive days where: $RR_{ij} \geq 1$ mm	Surface runoff recharge rate soil moisture
R95p (Equation (3))	Annual total PRCP when RR >95p. Let RR_{wj} be the daily precipitation amount on a wet day w (RR ≥1 mm) in period j and let $RR_{wn}95$ be the 95th percentile of precipitation on wet days in the base period. If W represents the number of wet days in the period, then: $R95\,p_j = \sum_{w=1}^{W} RR_{wj}$ where $RR_{wj} > RR_{wn}95$	Surface runoff rate, recharge rate
SDII (Equation (4))	Simple precipitation intensity index: Let RR_{wj} be the daily precipitation amount on wet days, w (RR ≥1 mm) in period j. If W represents number of wet days in j, then: $SDII_j = \frac{\sum_{w=1}^{W} RR_{wj}}{W}$	Surface runoff rate, recharge rate

mathematical calculations for the indices are well defined and performed using R; thus, the use of either software package should give similar results.

The indices were generated for each of the five Portland, OR rainfall stations spanning 1977–2005. The observed time series was shortened in this section to facilitate comparison with model simulation dates. The indices were generated from projections of the aforementioned five LOCA downscaled global climate models for historic (1977–2005) and future (2006–2100) periods for emissions scenarios RCP 8.5.

To detect change of each calculated ETCCDI index, the Mann–Kendall rank-based correlation test was selected and deployed. Several correlation tests exist and were considered. The Pearson correlation test was ruled out because the data were not normally distributed. The Spearman correlation test could have been selected as it is nearly equivalent to Mann–Kendall in practice (Yue *et al.* 2002). The Mann–Kendall test was selected because it was the preferred test of other researchers using ETCCDI calculations, which this research seeks to build on (Dumitrescu *et al.* 2015; Filahi *et al.* 2016). The Mann–Kendall test generates a tau and *p*-value to measure if there is a significant monotonic increase or decrease in a variable over time (Mann 1945). The tau value ranges between (−1, 1), and negative values indicate decreasing trends and positive values increasing trends. The significance level selected for this test was 10% (0.1) and 5% (0.05). The null hypothesis where *p*-value >0.1 indicates no significant monotonic trend exists. The test was performed using the Rv3.1.1 package 'Kendall' (McLeod 2015).

In order to satisfy the requirement of the Mann–Kendall test that data be independent, the indices were tested for autocorrelation. Tests of autocorrelation were completed using the partial autocorrelation function in R. Where autocorrelation was present, tau values were bootstrapped using the R package 'boot', which includes bootstrapping functions for autocorrelated time series data (Davison & Hinkley 1997; Canty & Ripley 2020). This test provides a mean tau value as generated by 500 instances of the Mann–Kendall function. Alternately, the R package 'bootstrap' may have been used. This package is also capable of

iterating functions such as the Mann–Kendall. However, the 'bootstrap' package is no longer recommended. The 'bootstrap' package is not documented thoroughly and is likely to produce user errors as it was developed to accompany a statistics training manual rather than general use (Tibshirani 1993).

Methods for Question 2: comparing annual and monthly trends

Comparing indices for different temporal units helps understand the limitations or benefits of annual analysis. By adding monthly analysis, a higher resolution picture of precipitation and temperature may be ascertained. A slight variation of methods from Methods 3.2.1 was made in part due to constraints in RClimDex. Different but comparable ETCCDI indices were selected from RClimDex based again on the representation of storm frequency and intensity (Table 4). Monthly indices include simple daily rainfall intensity (SDII), maximum 1 day event (Rx1day), maximum 5 day event (Rx5day), and total volume precipitation (PRCPTOT). Rx5day describes the persistence of rainfall in the place of CDD and CWD. Rx1day and PRCPTOT address the occurrence of single-day events and overall volume in the place of R95p. Two temperature indices were used, including maximum temperature (TXx) and minimum temperature (TNn) as these indicators have relevance in extrapolating more generally the implications of issues with temporal resolution.

Table 4 | Definition of ETCCDI indices used for research questions 2 and 3 (Karl *et al.* 1999; Peterson *et al.* 2001)

Indicator	Definition	Potential changes in the hydrological cycle
PRCPTOT (Equation (5))	Annual total precipitation in wet days: Let RR_{ij} be the daily precipitation amount on day i in period j. If i represents the number of days in j, then $\mathrm{PRCPTOT} = \sum_{i=1}^{I} RR_{ij}$	Runoff ratio
Rx1day (Equation (6))	Monthly maximum 1-day precipitation: Let RR_{ij} be the daily precipitation amount on day i in period j. The maximum 1-day value for period j are: $\mathrm{Rx1day}_j = \max(RR_{ij})$	Surface runoff rate
Rx5day (Equation (7))	Monthly maximum consecutive 5-day precipitation: Let RR_{kj} be the precipitation amount for the 5-day interval ending k, period j. Then maximum 5-day values for period j are: $\mathrm{Rx5day}_j = \max(RR_{kj})$	Surface runoff rate, recharge rate, soil moisture availability
SDII (Hourly) (Equation (8))	Hourly simple precipitation intensity index: Let RR_{wj} be the daily precipitation amount on wet days, w (RR $\geq$1 mm) in period j. If H represents number of wet hours in j, $\mathrm{SDII}_j = \frac{\sum_{w=1}^{W} RR_{wj}}{H}$	Surface runoff rate, recharge rate
TXx (Equation (9))	Monthly maximum value of daily maximum temperature: Let TX_x be the daily maximum temperatures in month k, period j. The maximum daily maximum temperature each month is then: $TX_{xkj} = \max(TX_{xkj})$	Evapotranspiration rate, soil moisture availability
TNn (Equation (10))	Monthly minimum value of daily minimum temperature: Let TN_n be the daily minimum temperatures in month k, period j. The minimum daily minimum temperature each month is then: $TN_{nkj} = \min(TN_{nkj})$	Evapotranspiration rate, soil moisture availability

Methods for Question 3: comparing daily versus and hourly data

For the last research question, the SDII index for rainfall intensity was examined using hourly data rather than daily data to determine the effect of high temporal resolution on trend detection. The ETCCDI formula for SDII uses daily rainfall totals, as given in Equation (4). The adapted formula to calculate SDII using hourly rainfall total is shown in Equation (8). Two calculations of SDII were therefore performed. All trends were analyzed with the Mann–Kendall and bootstrapping approach described in Question 1 methods. The null hypothesis of trend tests is that no monotonic trends exist.

RESULTS

Comparisons with downscaled global climate models using annual indices

No significant trends in Portland station observational records for 1977–2005 were found in precipitation indicators calculated annually. As shown in Figure 3(a), there are no significant trends from any of the four rain stations for 1977–2005. The record is shortened to mirror model simulation periods.

Consistent with the Portland observational record, few significant trends were detected from annual indices in

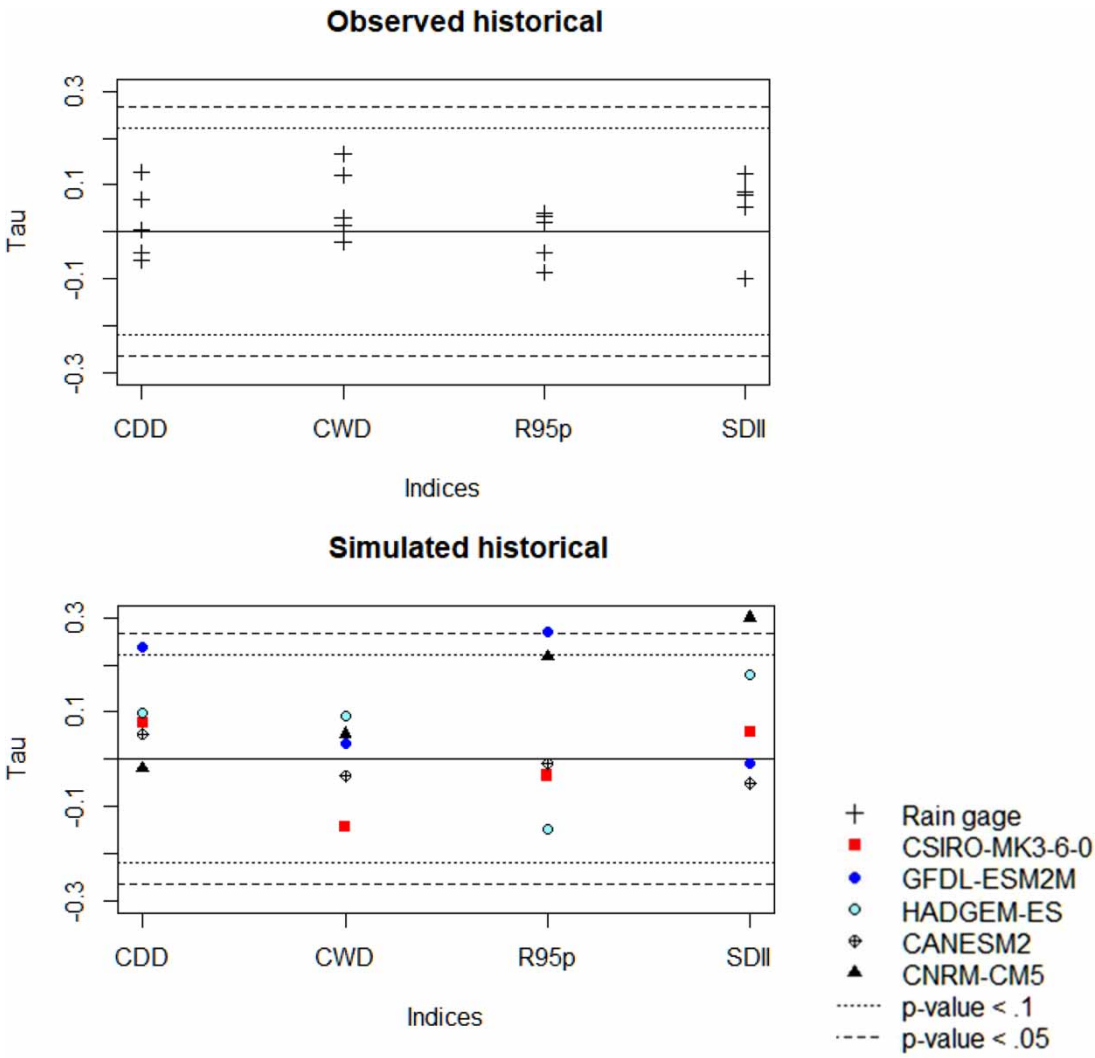

Figure 3 | Trends in annual indices from observations (a) and climate models (b) for 1977–2005.

precipitation projections for 1977–2005 from the LOCA downscaled global climate models. Figure 3(b) shows the results from the trend analysis of the projections. Three of the models did not show significant trends in any of the indices (CanESM2, HadGEM2-ES, CSIRO-Mk3.6.0). However, indices of CDD and R95p were significant in GFDL-ESM2M (tau = 0.24, 0.27, p-value = 0.07, 0.04) and SDII was significant in CNRM-CM5 (tau = 0.30, p-value = 0.03).

The climate models annual indices show projected precipitation trends for 2006–2100 are consistent with predictions that rainfall will be more intense in the Pacific Northwest. Figure 4 shows index trends from all models. Daily intensity (SDII) and heavy rain events (R95p) are both significant and increasing at the 5% significance level in three of the models (CanESM2, HadGEM2-ES, CSIRO-Mk3.6.0).

Overall CDD appears to increase with CWD models showing increase and decrease. The expected increase in CDD was significant in the CNRM-CM5 model (tau = 0.19, p-value = 0.01) and the HADGEM-ES model (tau = 0.12, p-value = 0.09). A significant increase in CWD was detected by the CanESM2 model (tau = 0.15, p-value = 0.04). In contrast, there was a decrease in CWD detected by the HADGEM2 (tau = −0.17, p-value = 0.02).

Historic simulations and observations using annual indices showed non-significant mixed direction trends. However, in future projections, multiple indices showed an intensified hydrologic cycle. As shown in Table 5, trends from these projections were mostly positive but not uniformly significant. Only the GFDL-ESM2M model projections showed no significant trends.

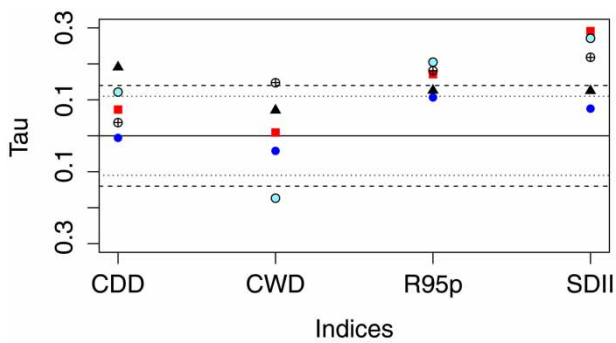

Figure 4 | Trends in annually calculated indices from climate models for 2006–2100.

Results for Question 2: comparing annual and monthly trends

Analysis of the observational data for 1977–2016 using annual indices PRCPTOT, Rx1day, Rx5day, and SDII indicate consistent increasing trends observed in only PRCPTOT, but no other precipitation indices (Figure 5). Temperature minimum index TNn is increasing and barely nonsignificant (tau = 0.18, p-value = 0.12). Temperature maximum index TXx is nonsignificantly decreasing (tau = −0.12, p-value = 0.28).

When examining precipitation indices on the monthly scale, a different picture emerges. Rx1day is increasing and significant in January and March at the 5% significance level (Figure 6(a)). Rx5day is increasing and significant in January, March, and June at the 10% significance level (Figure 6(b)). PRCPTOT is significant in March, October, and November at 5% significance (Figure 6(c)).

Table 5 | Comparison of trend directions, significance at 0.1 shown with filled triangles

	1977-2005 Models and Station Observations										2006-2100* RCP 8.5				
Index	CanESM2	CNRM-CM5	CSIRO-Mk3.6.0	GFDL-ESM2M	HadGEM2-ES	Station 4	Station 6	Station 10	Station 14	Station 58	CanESM2	CNRM-CM5	CSIRO-Mk3.6.0	GFDL-ESM2M	HadGEM2-ES
CDD	△	▽	△	▲	△	▽	△	△	△	▽	△	▲	△	▽	▲
CWD	▽	△	▽	△	△	△	△	△	△	▽	▲	△	△	▽	▼
R95p	▽	△	△	▲	▽	▽	△	▽	△	△	▲	▲	▲	△	▲
SDII	▽	▲	△	▽	△	△	△	▽	△	△	▲	▲	▲	△	▲

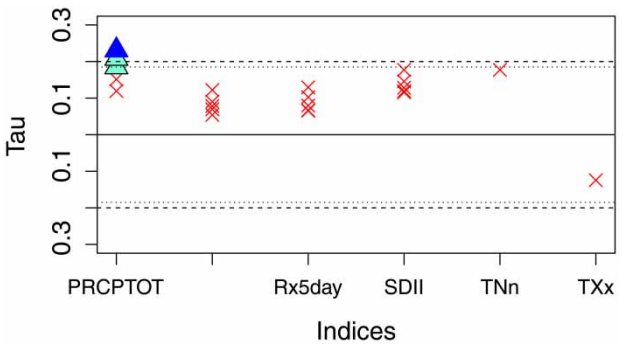

Figure 5 | Annual index trends for all rain gages and one temperature gage for 1977–2016.

Temperature variables also show departure from annual results (Figure 7). The index TNn is significantly increasing in summer months at 5%, while TXx is significant in none. A stepped pattern in the steepness of temperature increase is apparent in the temperature minimums where June, July, August, September, and October are all significant.

Results for question 3: comparing daily versus hourly scale

Comparison of monthly SDII at the daily and hourly scale indicates that the higher resolution detected many more trends. Monthly SDII at the daily scale is significant in January, March, and November (Figure 8(a)). Monthly SDII at the hourly scale is significant at 5% in January, March, April, October, and November (Figure 8(b)).

Results from autocorrelation testing showed that autocorrelation decreased as the period of study is decreased. At the annual scale, autocorrelation in annual PCRPTOT and SDII values was detected. Since only PRCPTOT was significant, bootstrapping was used to check the range of

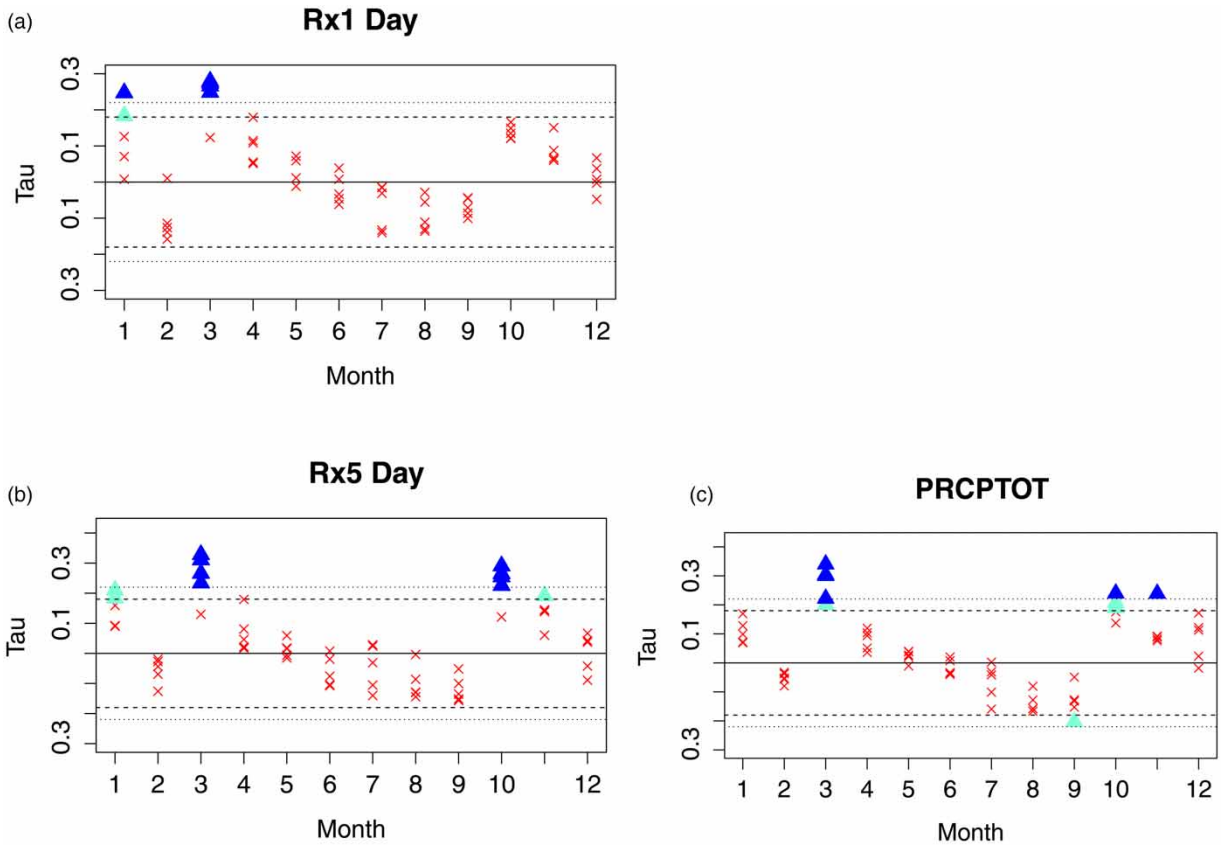

Figure 6 | Monthly index trends for Portland, OR observations for 1977–2016.

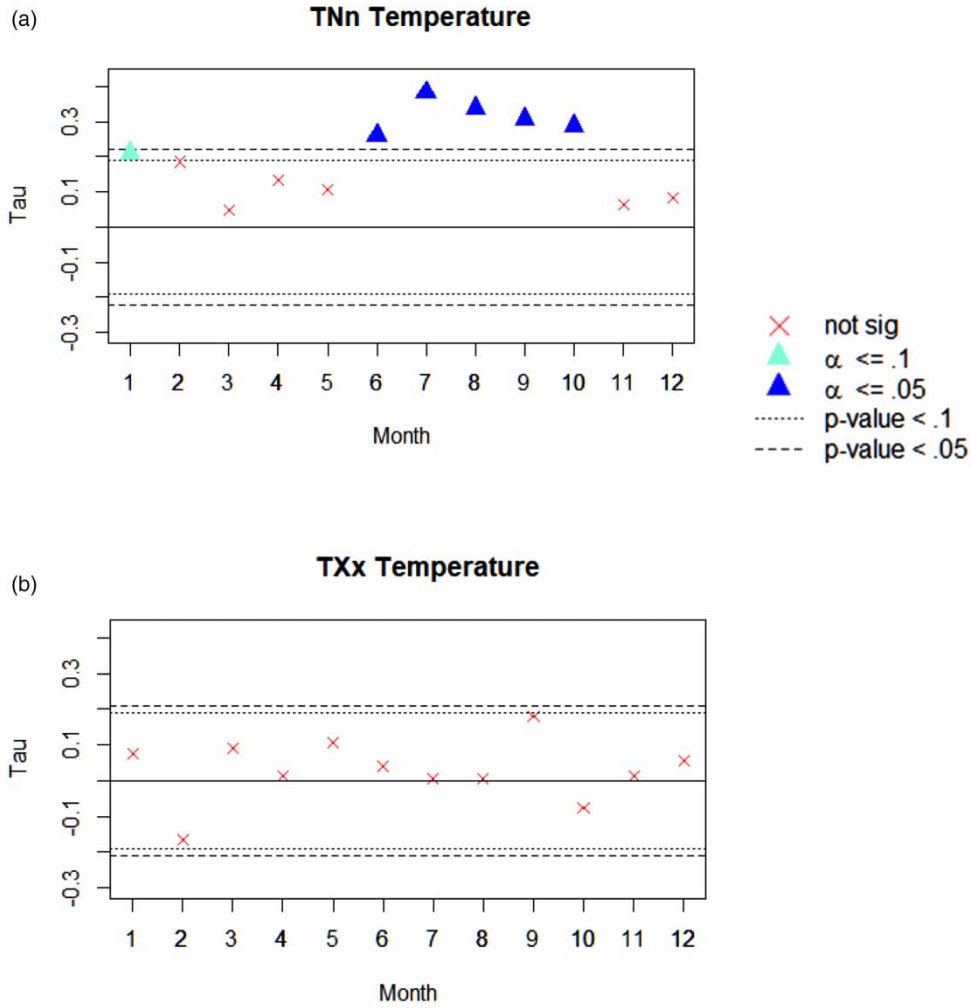

Figure 7 | Monthly index trends for Portland, OR observations for 1977–2016.

potential tau values for the station's autocorrelated data. Results indicated that tau values could range between positive and negative and that the increasing PRCPTOT tau values observed are subject to the possibility of false-positive detection (Kulkarni & von Storch 1995). Autocorrelation tests at the monthly scale showed that the strength of autocorrelation is minimal in PRCPTOT and removed entirely for SDII.

DISCUSSION

Changes to the hydrologic cycle are identified in the projected climate and not historic climate when trends are run on annual indices. Annual indices summarizing climate for 2006–2100 display increasing trends, indicative of an intensified hydrologic cycle in Portland, OR. The strongest index changes are apparent in the rainfall intensity and the total volume of rain from heavy rain events. The increase to consecutive dry is mostly positive as well, if less robust. This is consistent with the global analysis of climate projections characterizes future rainfall as more intense, with short-lived and heavy events amidst enduring dry periods (Giorgi *et al.* 2014).

Annual indices do not show increasing trends in data for the historical period of 1977–2005. This suggests that during this period, changes to rainfall have not been observed at the annual scale. The annual indices show

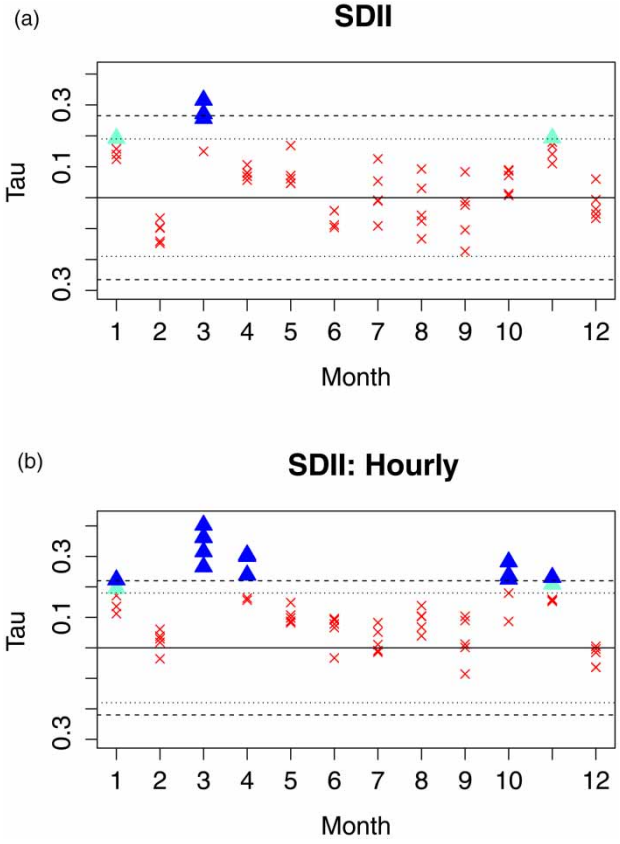

Figure 8 | Monthly index trends for Portland, OR observations for 1977–2016.

mixed directions in the signal of dry and wet spells. The change to CDD and CWD displays the largest disagreement between the models. One model (HadGEM2-ES) predicts an increase in dry spells and a decrease in wet spells. Another model (CNRM-CM5) shows increasing dry spells and no change to wet spells. The reverse trends were found in a third model (CanESM2). The various outcomes reflect possible atmospheric patterns projected for the future based on different assumptions in each model.

The hypothesis that wet spell length will decrease is based on simple principles that a warmer atmosphere is likely to be wetter and storms likely to be shorter and wetter. The possibility that wet spell length increases is proposed by other studies that show Pacific sea temperature rises contributing to an eastward shift of the North Pacific storm track, bringing longer wet spells to the US west coast (Kharin & Zwiers 2000). The lack of clarity is even attributed to the mid-latitude location of the Pacific Northwest, where Oregon is on the 45th parallel. The Canadian Global Coupled Model (CGCM1) indicates the mid-latitudes represent a gradient of change in western North America where southern areas experience a decrease in wet spell length and northern areas indicate an increase in wet spell length (Kharin & Zwiers 2000). The fact that our study area lies in the middle of the North American continent suggests there is considerable uncertainty in how the nature of wet spells will change; this is reflected by study results (Loikith *et al.* 2017).

Analysis of monthly precipitation characteristics in the City of Portland indicates the occurrence of more intense precipitation, heavier events, and a higher volume of monthly rainfall. These trends appear when indices are created monthly rather than annually. Higher intensity and heavier events are consistent with models. The rate of rainfall is expected to increase proportional to water vapor in a warming climate (Trenberth *et al.* 2003). Atmospheric rivers deliver vapor in traditionally cool months (Aragon *et al.* 2020). The observed increase to precipitation intensity occurs between October and March, thus increased vapor transport may be the physical mechanism driving trends. The higher volume of rainfall is not consistent with models. Global climate models project little change to Pacific Northwest annual mean precipitation during the twenty-first century (Mote & Salathé 2010). If mean precipitation goes unchanged and heavy rainfall increases, then moderate and light rainfall must decrease (Karl & Knight 1998). These decreases are not yet observed, suggesting that the observed changes to hydrology are the unfolding of a greater process. A possible explanation is that the increases in rainfall intensity are the first signals from climate change in precipitation and other signals are not yet affected.

The monthly indices reveal trends because they can capture changes to the seasons, while annual indices cannot. Trends showing changes to precipitation indices are concentrated in fall, winter, and spring months. Much of this can be attributed to atmospheric rivers. Recent studies show that the frequency of atmospheric rivers, which transport the vast amount of water vapor from the warm Pacific Ocean to western North America, have increased between 1979 and 2016 (Sharma & Dery 2020). In particular, atmospheric rivers are typically associated with extreme events and winter and fall heavy precipitation in Portland (Chen *et al.*

2018; Aragon *et al.* 2020). Simulation modeling shows that rainfall rates associated with atmospheric rivers are projected to increase in the Pacific Northwest at the beginning of the wet season (i.e., October) in the future (Shields & Kiehl 2016). In this study, trends appear in fall, winter, and spring. March has the highest concentration of observed precipitation change, including increases in intensity, volume, and single-day rainfall. The physical mechanisms generating spring change are unclear. In British Columbia, increase in spring storm intensity was also observed, but the area also experienced increased intensity in summer that is not apparent here (Jakob *et al.* 2003; Burn & Taleghani 2013).

Monthly analysis also revealed significant increases in temperature minimums not apparent at the annual scale. Minimum temperature increases are observed in all summer and early fall months. These increased temperatures may result in reduced condensation. However, decreasing trends in precipitation that may be expected to accompany surface warming were not yet apparent. Seasonal analysis of Portland rainfall and temperature records indicates that the area is experiencing precipitation change in fall, winter, and spring. Significant temperature change occurs in summer. It is worth considering that Portland's climate is temperate with a winter rainy season and dry summers. Increased energy inputs from global warming may act on precipitation in the rainy season but act directly upon air temperature in the dry season. The use of monthly indices allows for seasonal changes to be observed, which are not detected with annual indices.

The reliance on daily rainfall records in the ETCCDI methodology was shown to limit trend detection compared with hourly rainfall records. Daily scale records resulted in fewer significant trends than hourly scale records. At the 5% significance level, daily records were significant in March while hourly records were significant in more months including January, March, April, October, and November. This finding is consistent with expectations that daily scale records suppress intensity trend detection compared with hourly scale records (Cooley & Chang 2017). Compared to temperature, precipitation occurs at smaller spatial and temporal scales that are more difficult to measure (Boer *et al.* 2000). For this reason, gage spatial density and temporal resolution that is appropriate for temperature may not be appropriate for precipitation. The high spatial and temporal resolution of the data available in Portland's HYDRA network thus is an asset for the local area, although these trends cannot necessarily be extrapolated to the larger region. Analysis of Portland's gage network from 1977 to 2016 indicates that when precipitation indices are adapted to a higher temporal resolution and tested for monthly periods, a greater extent of hydrologic change can be observed.

Changes in the frequency, timing, and intensity of heavy precipitation events will have large consequences on the water cycle. However, the role of natural climate variability in these changes is unknown. Natural variability is thought to be responsible for an increase in mean precipitation observed in the Pacific Northwest over the twentieth century and may play a role in rainfall intensification (Mote 2003). Expanding this work to include more measures to evaluate observations against models could make this study more conclusive.

CONCLUSIONS

This study addresses the relationship between climate change and precipitation by examining how the lack of identifiable trends is affected by temporal resolution. ETCCDI indices that summarize precipitation characteristics at the monthly and annual levels are generated and tested for trends over the observed record and long-term future. The annual level indices demonstrate an intensifying hydrologic cycle from 2006 to 2100. These annually calculated indices do not show trends towards intensification in the observed record (1977–2005). However, when the indices are run to summarize data monthly instead of annually, trends showing intensification of the hydrologic cycle are apparent. Trend detection of increasing precipitation intensity became even more robust after the records themselves are moved from daily observations to hourly observations. The results demonstrate that the study of the effects of climate change on precipitation needs to reflect the ephemeral nature of rainfall. Signal change in precipitation patterns is likely to be obscured where annual characteristics such as annual mean rainfall are examined. Improving the resolution is likely to improve the change that important regional and seasonal changes are detected.

In seeking tools that use standard methodologies and are easy to understand for scientists and practitioners alike, the use of common indices like ETCCDI is of benefit. A reliance on annual summaries is a current limitation of the ETCCDI indices. Only a few parameters are available at the monthly scale, which makes the detection of seasonal changes difficult and therefore limits the detection of local and regional effects of climate change on precipitation. This limited availability represents a tradeoff between usability and accuracy. Several precipitation characteristics cannot be addressed at the annual scale. Still, the indices are based on daily observations that do allow places with simple observational networks to participate. Exploring additional indices that strike a balance to emphasize monthly and seasonal indices from daily observations would be an area for future study. Further, refining the performance measures by which indices are evaluated would allow for a more rigorous exploration of the success of these common metrics.

ACKNOWLEDGEMENTS

This work was supported by the Urban Resilience to Extremes Sustainability Research Network, NSF grant number SES-1444755. Additional support was provided by the Institute for Sustainable Solutions at Portland State University. Views expressed are our own and do not necessarily reflect those of sponsoring agencies. We appreciate anonymous reviewers who made helpful suggestions for improving the quality of the manuscript.

REFERENCES

Abatzoglou, J. T., Rupp, D. & Mote, P. W. 2014 Seasonal climate variability and change in the Pacific Northwest of the United States. *Journal of Climate* **27** (5), 2125–2142.

Aragon, C., Loikith, P. C., McCullar, N. & Mandilag, A. 2020 Connecting local-scale heavy precipitation to large-scale meteorological patterns over Portland, Oregon. *International Journal of Climatology*. doi:10.1002/joc.6487.

Barnett, T. P., Pierce, D. W., Hidalgo, H. G., Bonfils, C., Santer, B. D., Das, T., Bala, G., Wood, A. W., Nozawa, T., Mirin, A. A. & Cayan, D. R. 2008 Human-induced changes in the hydrology of the western United States. *Science* **319** (5866), 1080–1083.

Boer, G. J., Flato, G., Reader, M. C. & Ramsden, D. 2000 A transient climate change simulation with greenhouse gas and aerosol forcing: experimental design and comparison with the instrumental record for the twentieth century. *Climate Dynamics* **16** (6), 405–425.

Burgan, H. I. & Aksoy, H. 2020 Monthly flow duration curve model for ungauged river basins. *Water* **12** (2), 338.

Burn, D. H. & Taleghani, A. 2013 Estimates of changes in design rainfall values for Canada. *Hydrological Processes* **27** (11), 1590–1599.

Canty, A. & Ripley, B. 2020 *boot: Bootstrap R (S-Plus) Functions*. R package version 1.3-25. Available from https://cran.r-project.org/web/packages/boot/index.html.

Chang, H. 2007 Comparative streamflow characteristics in urbanizing basins in the Portland Metropolitan Area, Oregon, USA. *Hydrological Processes* **21** (2), 211–222.

Chang, H., Lafrenz, M., Jung, I.-W., Figliozzi, M., Platman, D. & Pederson, C. 2010 Potential impacts of climate change on flood-induced travel disruption: a case study of Portland in Oregon, USA. *Annals of the Association of American Geographers* **100** (4), 938–952.

Chang, H., Jung, I., Steele, M. & Gannett, M. 2012 Spatial patterns of March and September streamflow trends in Pacific Northwest streams, 1958–2008. *Geographical Analysis* **44** (3), 177–201.

Chen, X., Leung, L. R., Gao, Y., Liu, Y., Wigmosta, M. & Richmond, M. 2018 Predictability of extreme precipitation in western US watersheds based on atmospheric river occurrence, intensity and duration. *Geophysical Research Letters* **45** (21), 11693–11701.

Chou, C., Chen, C., Tan, P. & Chen, K. T. 2012 Mechanisms for global warming impacts on precipitation frequency and intensity. *Journal of Climate* **25** (9), 3291–3306.

Cooley, A. & Chang, H. 2017 Precipitation intensity trend detection using hourly and daily observations in Portland. *Oregon. Climate* **5** (1), 10.

Dai, A. 2011 Drought under global warming, a review. *Wiley Interdisciplinary Reviews: Climate Change* **2** (1), 45–65.

Dart, J. O. & Johnson, D. M. 1981 *Oregon, Wet, High and Dry*. Hapi Press, Portland, OR.

Davison, A. C. & Hinkley, D. V. 1997 *Bootstrap Methods and Their Application*, Vol. 1. Cambridge University Press, Cambridge.

de los Milagros, S. M., Brunet, M., Sigró, J., Aguilar, E., Groening, J. A., Bentancur, O. J. & Rojas, C. 2013 Warming and wetting signals emerging from analysis of changes in climate extreme indices over South America. *Global and Planetary Change* **100**, 295–307.

Dettinger, M. 2011 Climate change, atmospheric rivers and floods in California – a multimodel analysis of storm frequency and magnitude changes. *Journal of the American Water Resources Association* **47** (3), 514–523.

Diaz, F. L., Conde, C. & Sánchez, O. 2012 Analysis of indices of extreme temperature events at Apizaco, Tlaxcala, Mexico: 1952–2003. *Atmósfera* **26** (3), 349–358.

Dumitrescu, A., Bojariu, R., Birsan, M. V., Marin, L. & Manea, A. 2015 Recent climatic changes in Romania from observational

data (1961–2013). *Theoretical and Applied Climatology* **122** (1–2), 111–119.

Filahi, S., Tanarhte, M., Mouhir, L., El Morhit, M. & Tramblay, Y. 2016 Trends in indices of daily temperature and precipitations extremes in Morocco. *Theoretical and Applied Climatology* **124** (3–4), 959–972.

Giorgi, F., Lm, E. S., Coppola, E., Diffenbaugh, N. S., Gao, X. J., Mariotti, L. & Shi, Y. 2011 Higher hydroclimatic intensity with global warming. *Journal of Climate* **24** (20), 5309–5324.

Giorgi, F., Coppola, E. & Raffaele, F. 2014 A consistent picture of the hydroclimatic response to global warming from multiple indices: models and observations. *Journal of Geophysical Research: Atmospheres* **119** (20), 11695–11708.

Grimm, N., Blasquez, M. B., Chester, M., Cook, E., Groffman, P., Iwaniec, D. & McPhearson, T. 2018 *A Social-Ecological-Technical Systems Approach to Understanding Urban Complexity and Building Climate Resilience*. International Forum of Urbanism: Reframing Urban Resilience Implementation: Aligning Sustainability and Resilience, Barcelona, Spain.

Groisman, Y. P., Karl, T. R., Easterling, D. R., Knight, R. W., Jamason, P. F., Hennessy, K. J., Suppiah, R., Page, C., Wibig, J., Fortuniak, K., Razuvaev, V. N., Douglas, A., Førland, E. & Zhai, P.-M. 1999 Changes in the probability of heavy precipitation: important indicators of climatic change. *Climatic Change* **42** (1), 243–283.

Groisman, Y. P., Knight, R. W., Easterling, D. R., Karl, T. R., Hegerl, G. C. & Razuvaev, V. N. 2005 Trends in intense precipitation in the climate record. *Journal of Climate* **18** (9), 1326–1350.

Held, I. M. & Soden, B. J. 2006 Robust responses of the hydrological cycle to global warming. *Journal of Climate* **19** (21), 5686–5699.

Hense, A., Krahe, P. & Flohn, H. 1988 Recent fluctuations of tropospheric temperature and water vapour content in the tropics. *Meteorology and Atmospheric Physics* **38** (4), 215–227.

Homsi, R., Shiru, M. S., Shahid, S., Ismail, T., Harun, S. B., Al-Ansari, N., Chau, K.-W. & Yaseen, Z. M. 2020 Precipitation projection using a CMIP5 GCM ensemble model: a regional investigation of Syria. *Engineering Applications of Computational Fluid Mechanics* **14** (1), 90–106.

Huntington, T. G. 2006 Evidence for intensification of the global water cycle: review and synthesis. *Journal of Hydrology* **319** (1), 83–95.

Intergovernmental Panel on Climate Change (IPCC). 2013 *Contribution of Working Group I to the Fifth Assessment Report of the Intergovernmental Panel on Climate Change. Climate Change 2013: The Physical Science Basis*. Cambridge University Press, Cambridge, UK.

Jackson, R. B., Le Quéré, C., Andrew, R. M., Canadell, J. G., Korsbakken, J. I., Liu, Z., Peters, G. P. & Zheng, B. 2018 Global energy growth is outpacing decarbonization. *Environmental Research Letters* **13** (12), 120401.

Jakob, M., McKendry, I. & Lee, R. 2003 Long-term changes in rainfall intensities in Vancouver, British Columbia. *Canadian Water Resources Journal/Revue Canadienne Des Ressources Hydriques* **28** (4), 587–604.

Karl, T. R. & Knight, R. W. 1998 Secular trends of precipitation amount, frequency and intensity in the United States. *Bulletin of the American Meteorological Society* **79** (2), 231–241.

Karl, T. R., Nicholls, N. & Ghazi, A. 1999 CLIVAR/GCOS/WMO workshop on indices and indicators for climate extremes: workshop summary. *Climatic Change* **42**, 3–7.

Kharin, V. V. & Zwiers, F. W. 2000 Changes in the extremes in an ensemble of transient climate simulations with a coupled atmosphere–ocean GCM. *Journal of Climate* **13** (21), 3760–3788.

King, A. D., Klingaman, N. P., Alexander, L. V., Donat, M. G., Jourdain, N. C. & Maher, P. 2014 Extreme rainfall variability in Australia: patterns, drivers and predictability. *Journal of Climate* **27** (15), 6035–6050.

Klok, E. J. & Klein Tank, A. M. G. 2009 Updated and extended European dataset of daily climate observations. *Int. J. Climatol.* **29**, 1182. doi:10.1002/joc.1779.

Krishnamurthy, C. K., Lall, U. & Kwon, H. 2009 Changing frequency and intensity of rainfall extremes over India from 1951 to 2003. *Journal of Climate* **22** (18), 4737–4746.

Kruger, A. C. & Sekele, S. S. 2013 Trends in extreme temperature indices in South Africa: 1962–2009. *International Journal of Climatology* **33** (3), 661–676.

Kulkarni, A. & von Storch, H. 1995 Monte Carlo experiments on the effect of serial correlation on the Mann-Kendall test of trend. *Meteorologische Zeitschrift* **4** (2), 82–85.

Loikith, P. C., Lintner, B. R. & Sweeney, A. 2017 Characterizing large-scale meteorological patterns and associated temperature and precipitation extremes over the Northwestern United States. *Journal of Climate* **30**, 2829–2847.

Mann, H. B. 1945 Nonparametric tests against trend. *Econometrica: Journal of the Econometric Society* **13**, 245–259.

McLeod, A. I. 2015 *Kendall Rank Correlation and Mann-Kendall Trend Test*. R Package Kendall. Available from https://cran.r-project.org/web/packages/Kendall/Kendall.pdf

Moberg, A., Jones, P. D., Lister, D., Walther, A., Brunet, M., Jacobeit, J. & Alexander, L. V. 2006 Indices for daily temperature and precipitation extremes in Europe analyzed for the period 1901–2000. *Journal of Geophysical Research: Atmospheres* **111** (D22), D22106.

Mote, P. W. 2003 Trends in temperature and precipitation in the Pacific Northwest during the twentieth century. *Northwest Science* **77**, 271–282.

Mote, P. W. & Salathé Jr., E. P. 2010 Future climate in the Pacific Northwest. *Climatic Change* **102** (1–2), 29–50.

Munoz, E. A., Di Paola, D. & Lanfri, M. 2015 Advances on rain rate retrieval from satellite platforms using artificial neural

networks. *IEEE Latin America Transactions* **13** (10), 3179–3186.

Osborn, T. J., Hulme, M., Jones, P. D. & Basnett, T. A. 2000 Observed trends in the daily intensity of United Kingdom precipitation. *International Journal of Climatology* **20** (4), 347–364.

Panda, D. K., Panigrahi, P., Mohanty, S., Mohanty, R. K. & Sethi, R. R. 2016 The 20th century transitions in basic and extreme monsoon rainfall indices in India: comparison of the ETCCDI indices. *Atmospheric Research* **181**, 220–235.

Parker, L. E. & Abatzoglou, J. T. 2016 Spatial coherence of extreme precipitation events in the northwestern United States. *International Journal of Climatology* **36** (6), 2451–2460.

Peel, M. C., Finlayson, B. L. & McMahon, T. A. 2007 Updated world map of the Köppen-Geiger climate classification. *Hydrology and Earth System Sciences* **11**, 1633–1644.

Peterson, T. C. & Manton, M. J. 2008 Monitoring changes in climate extremes: a tale of international collaboration. *Bulletin of the American Meteorological Society* **89** (9), 1266–1271.

Peterson, T. C., Folland, C., Gruza, G., Hogg, W., Mokssit, A. & Plummer, N. 2001 *Report on the Activities of the Working Group on Climate Change Detection and Related Rapporteurs 1998–2001*. WMO, Geneva, Switzerland.

Pierce, D. W., Cayan, D. R. & Thrasher, B. L. 2014 Statistical downscaling using localized constructed analogs (LOCA). *Journal of Hydrometeorology* **15** (6), 2558–2585.

Praskievicz, S. & Chang, H. 2009 Winter precipitation intensity and ENSO/PDO variability in the Willamette Valley of Oregon. *International Journal of Climatology* **29** (13), 2033–2039.

Prein, A. F., Rasmussen, R. M., Ikeda, K., Liu, C., Clark, M. P. & Holland, G. J. 2016 The future intensification of hourly precipitation extremes. *Nature Climate Change* **7** (1), 48–52.

Rahimzadeh, F., Asgari, A. & Fattahi, E. 2009 Variability of extreme temperature and precipitation in Iran during recent decades. *International Journal of Climatology* **29** (3), 329–343.

R Core Team. 2014 *R: A Language and Environment for Statistical Computing*. R Foundation for Statistical Computing, Vienna, Austria.

Redmond, K. T. & Koch, R. W. 1991 Surface climate and streamflow variability in the western United States and their relationship to large-scale circulation indices. *Water Resources Research* **27** (9), 2381–2399.

Riahi, K., Rao, S., Krey, V., Cho, C., Chirkov, V., Fischer, G., Kindermann, G., Nakicenovic, N. & Rafaj, P. 2011 RCP 8.5 – a scenario of comparatively high greenhouse gas emissions. *Climatic Change* **109** (1–2), 33.

Rupp, D. E., Abatzoglou, J. T., Hegewisch, K. C. & Mote, P. W. 2013 Evaluation of CMIP5 20th century climate simulations for the Pacific Northwest USA. *Journal of Geophysical Research: Atmospheres* **118** (19), 10884–10906.

Rupp, D. E., Abatzoglou, J. T. & Mote, P. W. 2017a Projections of 21st century climate of the Columbia River Basin. *Climate Dynamics* **49** (5–6), 1783–1799.

Rupp, D. E., Li, S., Mote, P. W., Shell, K., Massey, N., Sparrow, S. N., Wallom, D. C. H. & Allen, M. R. 2017b Seasonal spatial patterns of projected anthropogenic warming in complex terrain: a modeling study of the western USA. *Climate Dynamics* **48** (7–8), 2191–2213.

Salathé, E. P. 2003 Comparison of various precipitation downscaling methods for the simulation of streamflow in a rainshadow river basin. *International Journal of Climatology* **23** (8), 887–901.

Salathé, E. P. 2006 Influences of a shift in North Pacific storm tracks on western North American precipitation under global warming. *Geophysical Research Letters* **33** (19), L19820.

Salathé, P., Hamlet, A. F., Stumbaugh, M., Lee, S. Y. & Steed, R. 2014 Estimates of 21st century flood risk in the Pacific Northwest based on regional scale climate model simulations. *Journal of Hydrometeorology* **15** (5), 1881–1899.

Sanò, P., Panegrossi, G., Casella, D., Di Paola, F., Milani, L., Mugnai, A., Petracca, M. & Dietrich, S. 2015 The passive microwave neural network precipitation retrieval (PNPR) algorithm for AMSU/MHS observations: description and application to European case studies. *Atmospheric Measurement Techniques* **8** (2), 837–857.

Seneviratne, S. I., Lüthi, D., Litschi, M. & Schär, C. 2006 Land–atmosphere coupling and climate change in Europe. *Nature* **443** (7108), 205–209.

Shamshirband, S., Hashemi, S., Salimi, H., Samadianfard, S., Asadi, E., Shadkani, S., Kargar, K., Mosavi, A., Nabipour, N. & Chau, K.-W. 2020 Predicting standardized streamflow index for hydrological drought using machine learning models. *Engineering Applications of Computational Fluid Mechanics* **14** (1), 339–350.

Sharma, A. R. & Dery, S. J. 2020 Variability and trends of landfalling atmospheric rivers along the Pacific Coast of northwestern North America. *International Journal of Climatology* **40** (1), 544–558.

Shields, C. A. & Kiehl, J. T. 2016 Atmospheric river landfall-latitude changes in future climate simulations. *Geophysical Research Letters* **43** (16), 8775–8782.

Soulis, E. D., Sarhadi, A., Tinel, M. & Suthar, M. 2016 Extreme precipitation time trends in Ontario, 1960–2010. *Hydrological Processes* **30** (22), 4090–4100.

Tangang, F., Juneng, L. & Aldrian, E. 2017 Observed changes in extreme temperature and precipitation over Indonesia. *International Journal of Climatology* **37** (4), 1979–1997.

Taylor, K. W., Stouffer, R. J. & Meehl, G. A. 2012 An overview of CMIP5 and the experiment design. *Bulletin of the American Meteorological Society* **93** (4), 485–498.

Thibeault, J. M. & Seth, A. 2014 Changing climate extremes in the Northeast United States: observations and projections from CMIP5. *Climatic Change* **127** (2), 273–287.

Tibshirani, R. 1993 Functions for the book 'An Introduction to the Bootstrap'. R version 2019.6.

Tohver, I. M., Hamlet, A. F. & Lee, S. Y. 2014 Impacts of 21st-century climate change on hydrologic extremes in the Pacific

Northwest region of North America. *Journal of the American Water Resources Association* **50** (6), 1461–1476.

Trenberth, K. E. 1998 Atmospheric moisture residence times and cycling: implications for rainfall rates and climate change. *Climatic Change* **39** (4), 667–694.

Trenberth, K. E. 2011 Changes in precipitation with climate change. *Climate Research* **47** (1–2), 123–138.

Trenberth, K. E., Dai, A., Rasmussen, R. M. & Parsons, D. B. 2003 The changing character of precipitation. *Bulletin of the American Meteorological Society* **84** (9), 1205–1217.

Turco, M. & Llasat, M. C. 2011 Trends in indices of daily precipitation extremes in Catalonia (NE Spain), 1951–2003. *Natural Hazards and Earth System Sciences* **11** (12), 3213–3226.

Wang, B., Luo, X., Yang, Y. M., Sun, W., Cane, M. A., Cai, W., Yeh, S. W. & Liu, J. 2019 Historical change of El Niño properties sheds light on future changes of extreme El Niño. *Proceedings of the National Academy of Sciences* **116** (45), 22512–22517.

Wentz, F. J., Ricciardulli, L., Hilburn, K. & Mears, C. 2007 How much more rain will global warming bring? *Science* **317** (5835), 233–235.

Xu, C., Widén, E. & Halldin, S. 2005 Modelling hydrological consequences of climate change – progress and challenges. *Advances in Atmospheric Sciences* **22** (6), 789–797.

Yue, S., Paul, P. & George, C. 2002 Power of the Mann–Kendall and Spearman's rho tests for detecting monotonic trends in hydrological series. *Journal of Hydrology* **259** (1–4), 254–271.

Zandonadi, L., Acquaotta, F., Fratianni, S. & Zavattini, J. A. 2016 Changes in precipitation extremes in Brazil (Paraná River basin). *Theoretical and Applied Climatology* **123** (3–4), 741–756.

Zhang, X. & Yang, F. 2004 RClimdex (1.0) user manual. *Climate Research Branch Environment Canada* **22** Downsview, Ontario, Canada.

Zhang, X., Zwiers, F. W., Hegerl, G. C., Lambert, F. H., Gillett, N. P., Solomon, S., Stott, P. A. & Nozawa, T. 2007 Detection of human influence on twentieth-century precipitation trends. *Nature* **448** (7152), 461–465.

Zhang, X., Alexander, L., Hegerl, G. C., Jones, P., Tank, A. K., Peterson, T. C., Trewin, B. & Zwiers, F. W. 2011 Indices for monitoring changes in extremes based on daily temperature and precipitation data. *Wiley Interdisciplinary Reviews: Climate Change* **2** (6), 851–870.

First received 29 February 2020; accepted in revised form 5 May 2020. Available online 11 June 2020